energies

Article

Two Generations of Hydrogen Powertrain—An Analysis of the Operational Indicators in Real Driving Conditions (RDC)

Ireneusz Pielecha [1,*], Andrzej Szałek [2] and Grzegorz Tchorek [3]

[1] Faculty of Civil and Transport Engineering, Poznan University of Technology, ul. Piotrowo 3, 60-965 Poznan, Poland
[2] Toyota Central Europe, ul. Konstruktorska 5, 02-673 Warszawa, Poland; andrzej.szalek@toyota-ce.com
[3] Faculty of Management, University of Warsaw, ul. Szturmowa 1/3, 02-678 Warsaw, Poland; grzegorztchorek@gmail.com
* Correspondence: ireneusz.pielecha@put.poznan.pl; Tel.: +48-61-224-4502

Abstract: Hydrogen fuel cells are systems that can be successfully used to partially replace internal combustion propulsion systems. For this reason, the article presents an operational analysis of energy flow along with an analysis of individual energy transmission systems. Two generations of the Toyota Mirai vehicle were used for the tests. The operational analyses were carried out on the same route (compliant with RDE test requirements), assessing the system's operation in three driving sections (urban, rural and motorway). Both generations of the drive system with fuel cells are quite different, which affects the obtained individual systems operation results as well as the overall energy flow. Research was carried out on the energy flow in the fuel cells, FC converter, battery and electric motor using a dedicated data acquisition system. The analyses were carried out in relation to the energy of fuel cells, battery energy and recovered braking energy. It was found that in the urban drive section of the second-generation system (due to its much larger mass), a slightly higher energy consumption value was obtained (by about 2%). However, in the remaining phases of the test, consumption was lower (the maximum difference was 18% in the rural phase). Total energy consumption in the research test was 19.64 kWh/100 km for the first-generation system compared to 18.53 kWh/100 km for the second-generation system. Taking into account the increased mass of the second-generation vehicle resulted in significantly greater benefits in the second-generation drive (up to 37% in individual drive sections and about 28% in the entire drive test).

Keywords: hydrogen powertrain; fuel cell; energy flow; battery; energy consumption

Citation: Pielecha, I.; Szałek, A.; Tchorek, G. Two Generations of Hydrogen Powertrain—An Analysis of the Operational Indicators in Real Driving Conditions (RDC). *Energies* **2022**, *15*, 4734. https://doi.org/10.3390/en15134734

Academic Editor: Albert Ratner

Received: 1 June 2022
Accepted: 25 June 2022
Published: 28 June 2022

1. Introduction

Modern exhaust emission limits mean that new, alternative sources of vehicle propulsion are in demand. A dozen or so years ago, natural gas provided hope for reducing exhaust emissions and reducing carbon dioxide emissions. However, it has become a fuel that only marginally reduces carbon dioxide emissions. At present, hydrogen fuel is the most rapidly developing fuel technology with minimal exhaust emissions and low CO_2 emissions [1]. Its use is now possible both in internal combustion engines [2] as well as in fuel cells [3,4]. Although internal combustion engines have been on the market for many years, their overall efficiency remains lower than that of a stack of fuel cells [5]. However, the technological costs are much higher for the current generations of fuel cells. Nevertheless, they are much more often perceived as the vehicle propulsion systems to be developed over the next several dozen years (not including electric vehicles).

The continuous development of fuel cell drives requires their analysis and further development. PEM cells (proton exchange membrane) are used in such vehicles. However, batteries already have a diverse design (nickel-metal hydride—Ni-MH or lithium-ion—Li-ion). The electrical capacity depends on the type of storage systems used. The need to optimize them makes it necessary to test such drives under different operating conditions.

Typical tests (homologation tests) are used very often, but tests under typical real traffic conditions are still the most in demand due to the greater consistency with the driving style of the driver. The present work deals with the evaluation of the energy flow in hydrogen propulsion.

2. Development of Hydrogen Technologies

Recent years have marked a huge advance for hydrogen in the economic and energy strategies of many countries around the world. The growing interest in hydrogen as fuel should be associated with increasing requirements due to the climate change setting high goals for minimizing air pollution and its main advantage: zero emissions. Hydrogen is also a reversible energy carrier and can be used for energy storage, which is particularly important when trying to create a dispersed energy grid relying heavily on renewable energy sources. For the above reasons, it has a chance to play an important role in the energy transformation and decarbonization of many sectors—energy, heating, heavy industry and transport.

However, one of the key challenges faced by the representatives of various industries is the maturity and availability of various hydrogen-based technologies as a means of reaching a neutral environmental impact. However, as the estimates of the International Energy Agency suggest, currently, only about 30% of technologies in operation that are needed to achieve climate neutrality are mature and ready. The remaining 70% are technologies still in the prototype or demonstrator phases that have not yet been implemented on a significant scale [6]. It is, therefore, interesting to look at the readiness assessment of hydrogen technologies, including their applications in transport.

It means that so-called learning rates will determine the pace of convergence towards highly efficient technologies ready to serve hydrogen economy. While the passenger car market is traditionally seen as an innovation driven industry, it can also spur a lot of spillovers to other industries. In this context, it would be valuable to assess what is the current level of the technical readiness of the hydrogen technologies in automotive transportation and what is the estimated learning rate for an integrated hydrogen technology system, namely the hydrogen car.

Based on original and unique research conducted as a background of the Polish Hydrogen Strategy, we used TRL (Technology Readiness Level) and CRI (Commercial Readiness Index) classifications to assess the level of development and implementation of hydrogen technologies. The first of them, developed in the 1970s by NASA, allows for the assessment of the technology's maturity for its commercial application, grading its development from TRL 1, basic research, to TRL 9, technology proven in real conditions. The second method of classification relates to the implementation of the technology on the market, taking into account the number and variety of its applications. The CRI scale is stretched between the CRI 1 value, which means the possibility of the technology's hypothetical use, and the CRI 6 value, which means its widespread recognition, application and popularization, allowing it to become a universal asset that may be part of a financial institution's collateral. The CRI classification has been applied by the Australian Renewable Energy Agency (ARENA) to implement public support for particular technologies.

Both of these classifications, TRL and CRI, are used increasingly more often in literature as complementary methods of a technology's maturity and dissemination assessment, including low- and zero-emission technologies [7–9]—see Figure 1.

An analysis determining the knowledge base performed for the Polish Hydrogen Strategy has provided the research results shown below. The research process was carried out in April and May 2021 and consisted of steps including extensive consultation with stakeholders in expert panels (about 100 experts—including both domestic and foreign), in-depth interviews (16) and a survey on a sample of 30 specialists. The study, in its scope, covered all of the elements of the hydrogen economy value chain—production, storage, transport, distribution and use of hydrogen. However, since this article focuses on issues of transport and mobility, the cited TRL and CRI results were assessed selectively for the use of hydrogen in various modes of transport.

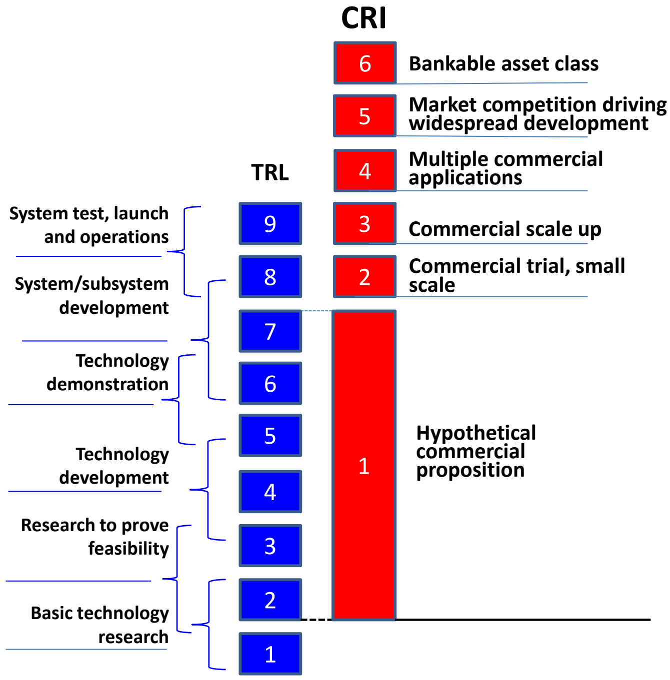

Figure 1. The TRL and CRI classification types [10].

When asked about the overall level of hydrogen technologies available in the world, experts indicated that among the solutions mentioned in the field of transport applications, the highest level of TRL can be observed for solutions in passenger vehicles and city buses. The same applies to the results using the CRI level.

According to intuition, the lowest level of currently assessed technological readiness and commercialization concerns the use of hydrogen in the field of commercial aviation and large sea-going vessels—see Figure 2.

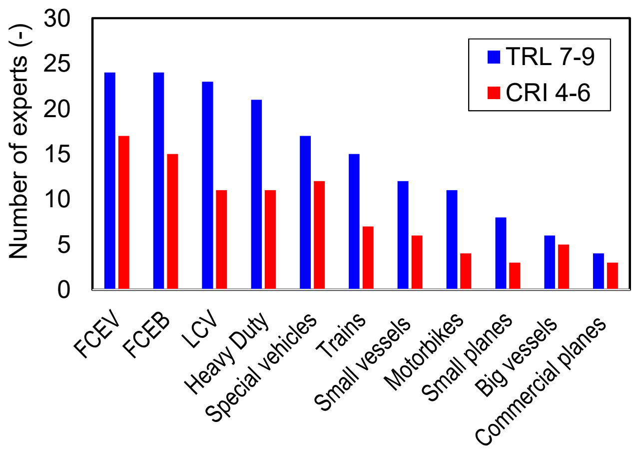

Figure 2. Assessment of the TRL and CRI levels for hydrogen technologies in transport solutions [11] (TRL 7–9 indicates the number of experts who determined a given technology/application to qualify as TRL 7, TRL 8 or TRL 9 in the TRL classification; CRI 4–6 indicates the number of experts who determined a given technology/application to qualify as CRI 4, CRI 5 or CRI 6 in the CRI classification); FCEV—fuel cell electric vehicle, FCEB—fuel cell electric bus, LCV—light commercial vehicle.

The above-mentioned observations are also correlated with the prospect of implementing individual technologies in Poland in the coming years. Respondents were asked about the period in which to expect the widespread use of hydrogen technologies in mobility: 2021–2025, 2026–2030, 2031–2035, 2036–2040 (Figure 3). Compared to the use of hydrogen technologies in other areas of the value chain, mobility and transport seems to be a leader with a clear presence in passenger vehicles and buses [12].

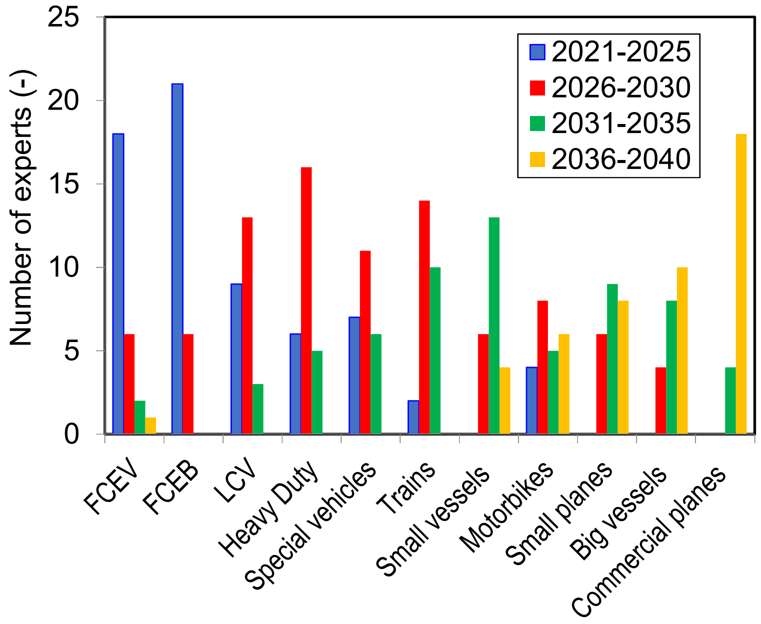

Figure 3. Time perspective for the implementation of hydrogen technologies in mobility [11].

3. Fuel Cell Testing for Automotive Applications

The automotive fuel cell market began to grow in 2014 in the U.S. Official U.S. sales of Hyundai's cars began in June 2014, Toyota's in October 2015 and Honda's in December 2016 (primarily in the state of California) [13].

The modern development of hydrogen propulsion systems is mainly centered around Toyota and Hyundai vehicles. The second-generation Toyota Mirai is the equivalent of the second-generation Hyundai Nexo. Despite belonging to a different segment of vehicles (sedans and SUVs, respectively), these vehicles have fuel cells with a power of about 100 kW (128 kW vs. 95 kW) and batteries with similar parameters (1.24 kWh vs. 1.56 kWh) [14].

A comparative analysis conducted by Jiao et al. [15] leads to the conclusion that, based on the example of the Toyota Mirai, the power density of the fuel cell stack has increased. The first generation of this drive reached a value of about 3 kW/dm^3 (MY2014), while the second generation was at 4.4 kW/dm^3 (MY2020; these values include end plates—the values may be higher otherwise). End plates play a critical role in the overall process of fuel cell optimization, as evidenced, for example, by the work of Habibnia et al. [16]. Current density in subsequent generations of Toyota Mirai propulsion was increased by 15% [17]. The European Union Fuel Cells and Hydrogen Joint Undertaking (EU-FCH JU) recently demonstrated a PEMFC stack with a power density of 5.38 kW/dm^3 (with end plates) at a current density of 2.67 A cm^{-2} and a single-cell voltage of 0.6 V [18]. The goal is to reach 9.3 kW/dm^3 by 2024 [19].

Research on fuel cells operation is carried out both in terms of simulation analyses and actual tests on real vehicles.

Fuel cell simulation studies are performed with relation to the high degree of interactions between the fuel cell's internal humidity management as well as the anode circuit and the temperature control strategy [20]. Similar studies are conducted in the field of two-dimensional [21,22] or three-dimensional [23–25] fuel cell analyses.

The authors conducted experimental studies on a miniature fuel cell system with a power of 30 W [26]. The research analyzed the cooperation between the fuel cell and the

NiMH battery under various vehicle driving conditions. With low dynamics of travel, the use of the fuel cell was about 50%, while with high dynamics, the use was about 25%.

Research on the Toyota Mirai drive system is also carried out in the field of simulation analyses. The degree of drive hybridization analysis was conducted out by de Almeida and Kruczan [27]. Analyses were made regarding the selection of the fuel cell stack and the size of the battery. It was found that a high degree of hybridization (HF = 70%) results in advantages in the propulsion characteristics and reduces the vehicle cost. Research by Loshe-Busch et al. [28] concerned Mirai MY2016 tests on a chassis dynamometer, taking into account various thermal conditions. It was found that energy consumption (in the UDDS test) at −7 °C ambient temperature was 157% higher than at +25 °C. Experimental research conducted at the Argonne National Institute concerned dynamometer tests in various American vehicle test procedures. The efficiency of the fuel cell stack was found to be 66%, and the overall drive system efficiency was at 63.7% [29].

The analysis of fuel cell degradation in typical tests was carried out by Raeesi et al. [30]. The degradation of the cells in both the NEDC and the FTP75 tests was found to lead to an increase in hydrogen consumption of about 14%. Changizian et al. [31] also optimized the performance of fuel cells together with batteries and ultracapacitors in driving tests. The use of an ultracapacitor resulted in a reduction in hydrogen consumption of about 3% and a reduction of about 20% in the different starting and end positions. Investigations of fuel cells under real traffic conditions were investigated by Ferara et al. [32] for heavy duty vehicles and Xu et al. [33] for buses. There are many fuel cell studies in the type approval tests, but there is no RDE-based analysis of passenger cars under real traffic conditions.

The authors carried out earlier research on the analyzed drive type only using the first version of the Toyota Mirai drive system [34]. These studies showed a low degree of hybridization, as the fuel cells held over 70% of all available energy.

As the presented analyses and results show, no road tests correspond to the current requirements of drive tests—especially European ones. Therefore, it is particularly important to carry out road tests, which correspond much more accurately to real driving during typical vehicle operating conditions. The authors follow the guidelines of the RDE test requirements. This means that the tests of both drive generations meet the requirements of the test. This test shows the requirements for driving time, speed, acceleration and length of the individual driving times. For each of these indicators, however, there are ranges in which the results should flow. All these requirements have been met. The innovative power of research lies in the representation of actual energy flows under normal traffic conditions. Driving tests still do not represent the typical conditions and fuel and energy consumption of hybrid (exhaust or hydrogen) or electric systems.

4. Materials and Methods

The drive systems tests were conducted on two generations of Toyota (Toyota, Japan) Mirai (first generation—MY2014 and second generation—MY2021). The first generation used hybrid drive components (the energy management unit and the electric motor come from a Lexus (Nagoya, Japan) RX 450 h model and the battery from a Toyota Camry). The second generation of the vehicle is a different design. Changes were introduced in it that influence the operating parameters of the drive system, including fuel cell with higher power (+11%) and higher energy density (+42%), electric motor with higher power (+8%) with a lower maximum torque value (−10%). The technical data of both models have been presented in Table 1. The fuel cell with which the vehicle was equipped had a smaller number of cells, but at the same time, had more power. Three (instead of two) hydrogen tanks with increased hydrogen mass (+18%) were installed, which allowed (despite the increased vehicle mass by 23%) to increase the range by about 25%.

Table 1. Toyota Mirai powertrain system [17,35].

Component	Parameter	Mirai I Gen.	Mirai II Gen.
Vehicle	mass	1850 kg	2415 kg
	top speed	179 km/h	175 km/h
	acceleration 0 to 60 mph	9.6 s	9.2 s
	range (homologation cycle)	approx. 483 km	650 km
Fuel cell	type	PEM (polymer electrolyte)	
	power	114 kW (155 KM)	128 kW (174 KM)
	power density	2.8 kW/kg; 3.5 kW/dm^3 (excl. end plates)	5.4 kW/kg; 5.4 kW/dm^3 (4.4—incl. end plates)
	number of cells	370	330
Electric motor	type	permanent magnet synchronous	
	peak power	123 kW at 4500 rpm	134 kW at 6940 rpm
	maximum torque	335 Nm	300 Nm at 0–3267 rpm
	Maximum speed	13,500 rpm	16,500 rpm
Battery	type	Nickel Metal Hydride (NiMH)	Li-Ion
	capacity	6.5 Ah	4 Ah
	output	25.5 kW × 10 s	31.5 kW × 10 s
	nominal voltage	244.8 V (7.2 V × 34)	310.8 V (3.7 V × 84)
	energy	1.59 kWh	1.24 kWh
	mass	46.9 kg	44.6 kg
Hydrogen storage	internal volume	122.4 dm^3	142.2 dm^3
	nominal pressure	70 Mpa	70 Mpa
	mass	4.6 kg	5.6 kg

Table 1 shows the main differences between the two drive generations. Mechanically, the systems do not differ from each other. The differences mainly concern other fuel cell, electric motor and battery solutions. The biggest mechanical difference is in the number of hydrogen tanks: two in the older generation and three in the newer generation. For this reason, only the changes in the number of hydrogen tanks in vehicle systems are shown in Figure 4.

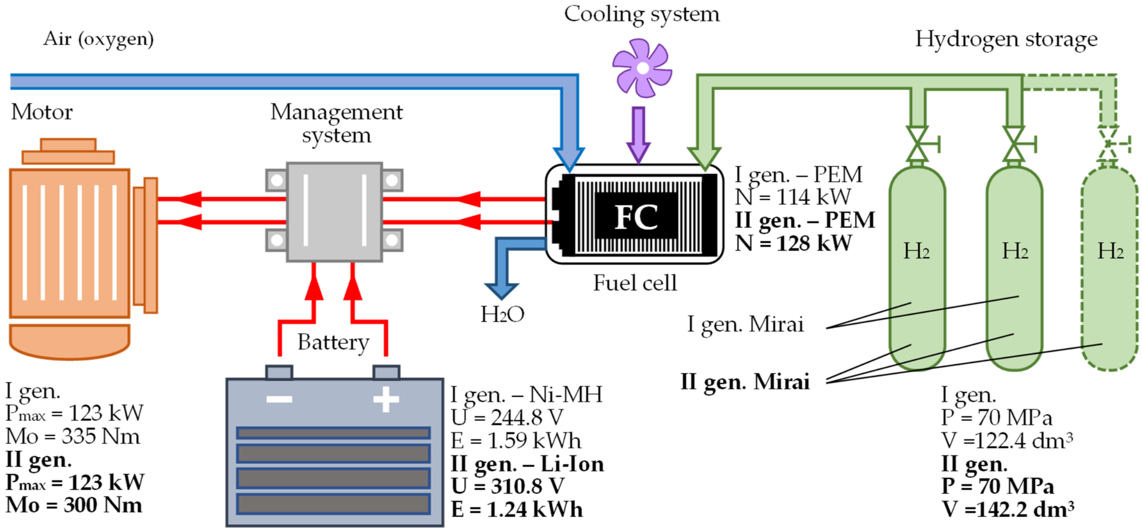

Figure 4. Diagram of the two drive generations analyzed in the article.

The exact scope of the research and its analyses is shown in Figure 5. The hybrid drive tests were carried out with the use of appropriate research equipment—a dedicated diagnostic tester—Techstream. Measurements that were made included: (a) mechanical (vehicle speed) and braking conditions with the use of an electric motor, (b) voltage and current of the battery and other characteristic values necessary to determine the energy flow in the drive system. Measurements of battery voltage and current, as well as changes in the battery SOC, were compared with the driving conditions in individual test phases to determine the conditions corresponding to the measured energy flow in the drive system. The data acquisition resolution was 1 Hz, which was a sufficient value to also analyze the driving conditions in the RDC test. Therefore, the necessary diagnostic data to determine the performance and energy of batteries and fuel cells were collected. In addition, the braking energy is specified. The benchmarking analysis allows a complete evaluation of the two powertrain generations under real traffic conditions.

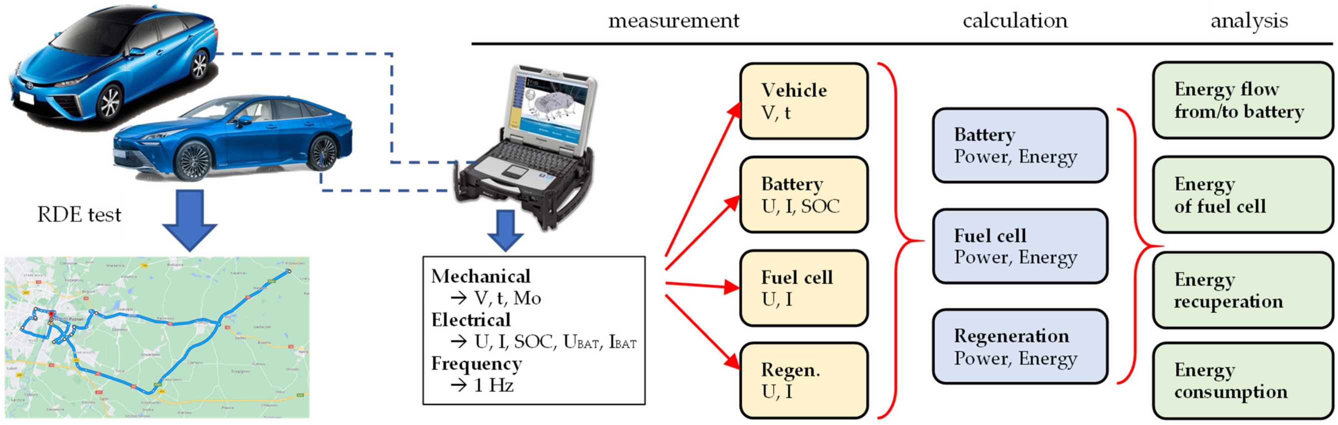

Figure 5. Information flow diagram for the determination of energy flow indicators for the analysis of fuel cell drive generations.

Using the measurement data presented above, the following quantities were determined:

- Energy flow (for urban, rural and motorway sections):

$$\Delta E_i = \int_{t=0}^{t=t_{max}} U_{BAT} \cdot I_{BAT} dt \tag{1}$$

where the instantaneous energy flow values ΔE_i were divided according to the following criteria:

- Discharging (for urban, rural and motorway sections):

$$\Delta E_{dis} = \int_{t=0}^{t=t_{max}} U_{BAT} \cdot I_{BAT} dt \text{ (if } \Delta E_i < 0), \tag{2}$$

- Charging (for urban, rural and motorway sections):

$$\Delta E_{ch} = \int_{t=0}^{t=t_{max}} U_{BAT} \cdot I_{BAT} dt \left(\text{if } \Delta E_i > 0 \text{ and } T_{reg} \geq 0\right), \tag{3}$$

- Regenerative braking (for urban, rural and motorway sections):

$$\Delta E_{reg} = \int_{t=0}^{t=t_{max}} U_{BAT} \cdot I_{BAT} dt \left(\text{if } \Delta E_i > 0 \text{ and } T_{reg} < 0\right), \tag{4}$$

where U_{BAT}—voltage (V), I_{BAT}—current (A), dt—time interval (h) and T_{reg}—braking torque (Nm);

- Boost value (for urban, rural and motorway sections):

$$\text{boost} = \frac{U_{HV}}{U_{LV}} \tag{5}$$

where U_{LV}—low voltage side (V) and U_{HV}—high voltage side (V);

- Specific energy (for urban, rural, and motorway sections):

$$E_m = \frac{E_i}{m} \quad (6)$$

where m—vehicle mass.

5. Results

5.1. Driving Test Evaluation

The road tests were all carried out on the same route, which was in line with the RDE test conditions (exhaust emission measurements were not performed as the testing only focused on the energy flow in the vehicle drive system). The tests were performed and repeated within a period of 4 months (April–August). The research results did not indicate any relationship between the changing atmospheric conditions and the measured values of the energy flow in the drive system.

The road driving test characteristic (Figure 6) shows that the two drive cycles were very similar. In accordance with the test procedure requirements, urban, rural and motorway travel sections were carried out (in that order). The second drive section was about 350 m longer (0.33% of the difference). However, the DRE test guidelines were all still met (including a limit of 120 min of test duration). Additionally, all of the requirements related to the share of the individual test phases duration were complied with (these requirements are included in Figure 6).

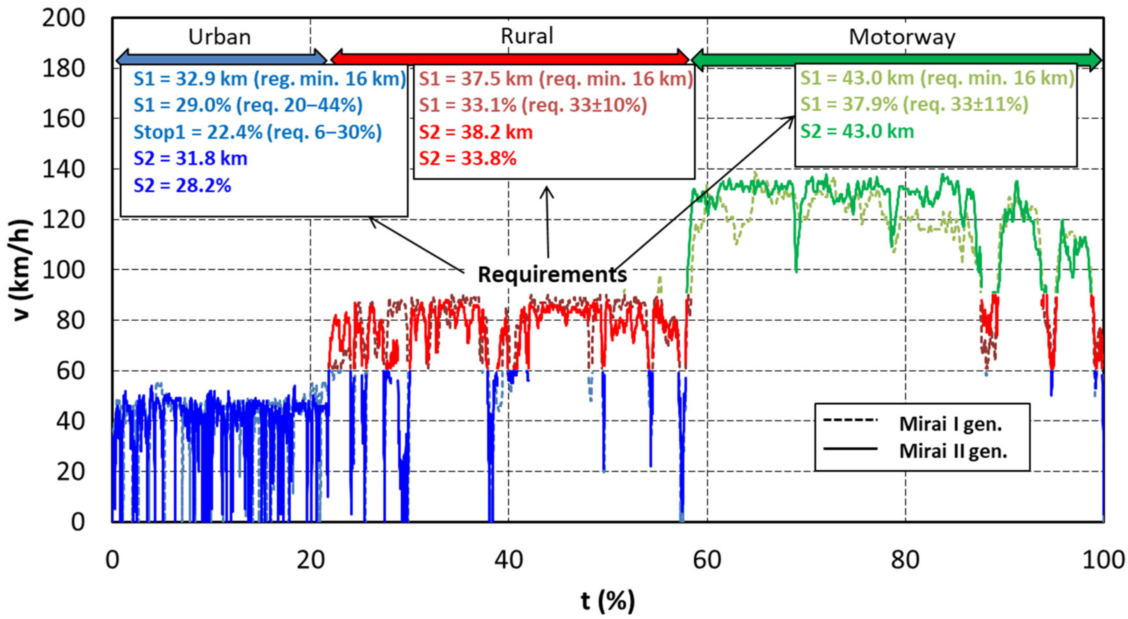

Figure 6. Comparison of speed profiles during two test drives of first-generation Mirai (dashed line) and second-generation Mirai (solid line).

The high similarity of the speed profiles enables a comparative analysis of the obtained test results of two generations of drives equipped with hydrogen fuel cells.

5.2. State of Charge (SOC)

The initial and final SOC values for the first- and second-generation vehicles were 57.2/59.21 and 52.15/67.45, respectively. The SOC change was also, respectively, 7% and 15% in favor of the second-generation vehicle. The maximum SOC values while driving were 60 and 67.45%, respectively. This means that the maximum SOC value for the second-generation Mirai was also the final value (Figure 7).

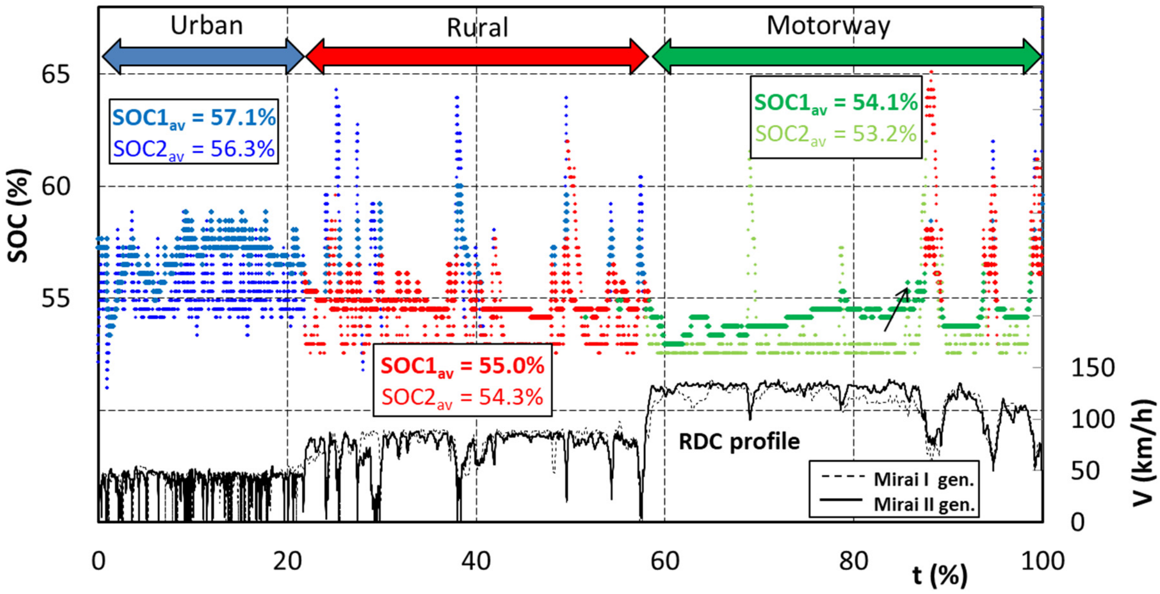

Figure 7. The batteries SOC changes against the speed profiles of both generations of Toyota Mirai (bigger dots—first generation; smaller dots—second generation).

The analysis of SOC changes indicates much higher values obtained in the second-generation drive. This is mainly due to this drive generation using a modern Li-ion battery. Vehicle braking increases the overall braking energy and also its ability to accumulate in the battery. The change in the number of brakes results from the real traffic conditions. At the same time, energy storage can be increased due to the higher vehicle weight and other battery types (Li-ion instead of Ni-MH). The peaks of SOC changes in Figure 6 indicated a large variation in SOC during driving. A characteristic feature is the fact that for both vehicles—as the test phases changed—the mean SOC value was reduced. These changes are not significant and amount to 2% for both generations. The addition of a Li-ion battery also has another advantage—it enables greater discharge capabilities of the battery system. In the range of SOC = 53–54%, the second generation of the drive works much more frequently.

A detailed analysis of the battery SOC shows very similar shares of vehicle speed values in both test drives (Figure 8—upper charts). In urban and rural drive sections, the same profiles of the driving speeds share were obtained. Some differences were observed for motorway driving, in which there was a notably greater share of speed in the range of 131–140 km/h (when driving the second-generation vehicle). These changes were not a result of the difference between vehicle generations, but rather from the congestion level of motorway traffic.

SOC changes depend on the type of battery used (Ni-MH type in the older generation, Li-ion in the newer). Although the second-generation drive had a lower capacity battery (4 Ah compared to 6.5 Ah), the actual usable capacity utilization range was 29% greater. This is due to a 16% change in SOC, compared to the 7% change with the first-generation drive. Similarly, if one takes into account the energy stored in the battery (with the linear relation of its changes), the change of capacity was 46% greater. This is due to, as mentioned previously, the changes in SOC (first generation—0.1113 kWh to 0.198 kWh in the second generation of the drive). The higher battery voltage in the second-generation drive means that the maximum power of this system was 31.5 kW (for 10 s), which is a value 20% higher than the power of the battery in the first-generation vehicle. Despite the newer battery system type and a lower energy capacity, the new vehicle mass has been reduced by only 5%.

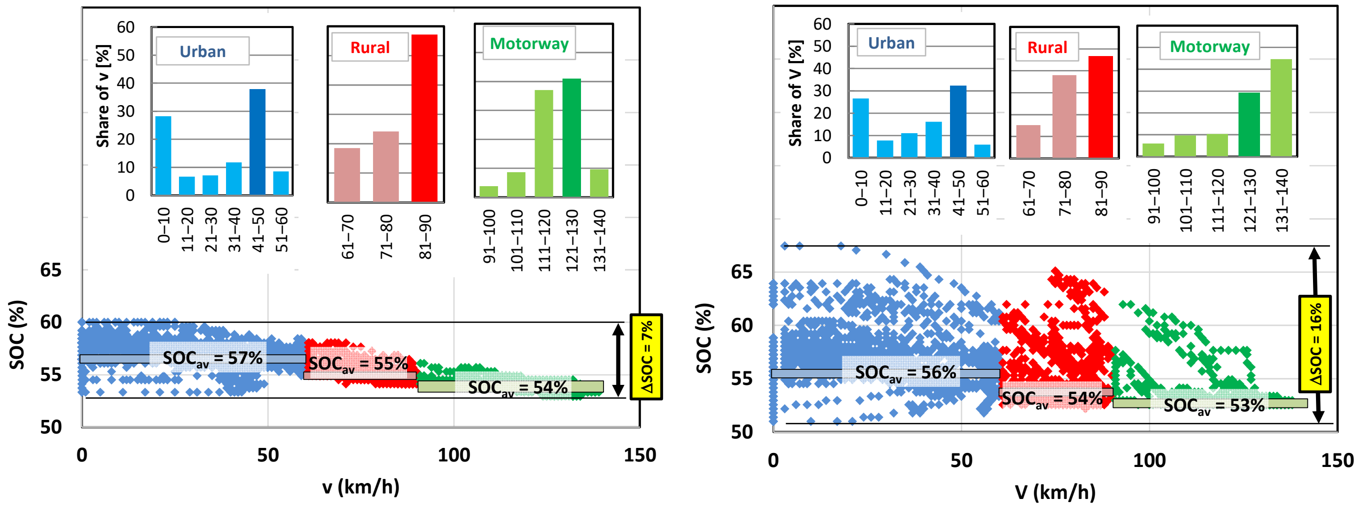

(**a**) (**b**)

Figure 8. Interval analysis of SOC relative to the vehicle driving speed with the shares of the selected speed intervals: (**a**) for the first generation; (**b**) for the second-generation Toyota Mirai.

5.3. Powertrain Performance Evaluation

SOC variations of different battery types have an impact on the charging and discharging power of the batteries.

Despite the different nominal voltage values (Figure 9), the current intensity values were similar. They oscillated around 100 A during operation (when the battery was discharging) and also 100 A during its charging. The discharging values were slightly higher for the older generation of batteries and for the newer generation during charging. The nominal voltage values in a Ni-MH battery (first-generation Mirai) were practically the minimum values of this voltage (Figure 9a). When the battery was discharged, the supply voltage assumed a range of 244–300 V. Charging the battery causes these voltages to be higher, reaching a range of 260–320 V. The maximum power analysis showed that its values are the highest during battery charging (Ne-max = 32.7 kW). The maximum value of Ne = 26.2 kW was recorded for discharging. This was 20% less than the value obtained for charging.

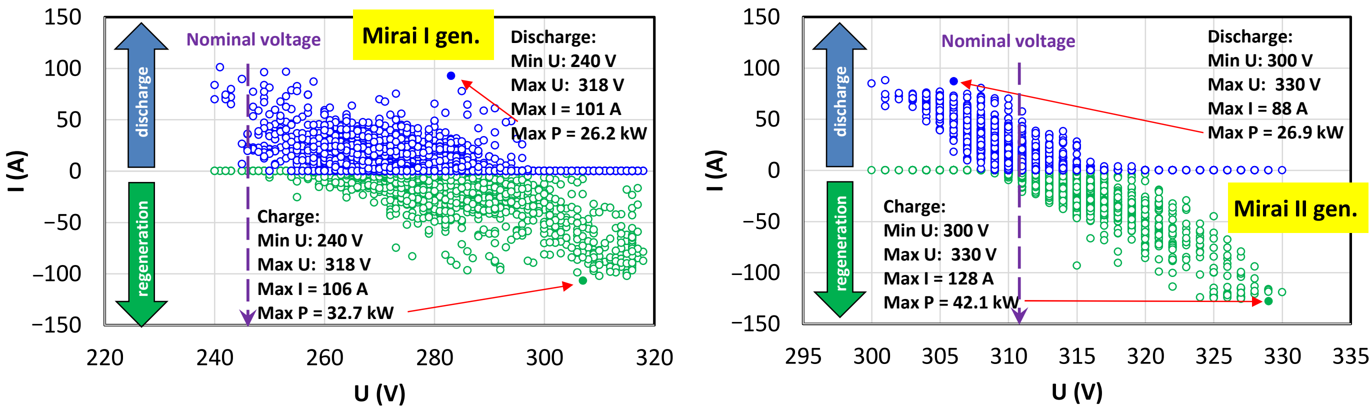

(**a**) (**b**)

Figure 9. Battery charging and discharging characteristics: (**a**) for the first-generation Toyota Mirai; (**b**) for the second-generation Toyota Mirai.

The second-generation vehicle drive was equipped with a Li-ion battery with a nominal voltage of 311 V (Figure 9b). This value was the minimum value when charging (the range achieved was 310–330 V). During battery discharge, lower voltage values in the range of 300–320 V were obtained). Despite different voltage values in the first- and second-generation systems, the achieved discharge powers were similar (in the second generation, the maximum value was 26.9 kW). Higher values were recorded during battery charging, i.e., 42.1 kW, which was 27% higher in relation to the first generation of the battery. The Li-ion battery also has a much narrower range of battery voltage changes, which amounts to U = 30 V. In the older version, the range of changes was 80 V (which is over 160% of the voltage range of the Li-ion battery).

5.4. EV and FC Operation an Energy Consumption

Modifying the fuel cell stack in the next generation of vehicle propulsion increased power by 20%. At the same time, the cell width was reduced from 1.34 mm to 1.1 mm by reducing the width of the separator (from 0.13 to 0.1 mm) and reducing the number of flow channels from 3 to 2 [17]. Thanks to these measures, the size of the stack of cells were reduced from 33 to 24 dm^3 and their mass from 41 to 24 kg—excluding the end plates; as a result, the number of cells was reduced from 370 to 330.

The analysis of the voltage and current relationship of the fuel cell stack (Figure 10) showed similar values for the generated voltage (in the range of 300–650 V). Additionally, in the first generation, single-area changes in voltage amplification were observed. In the second-generation solution, two independent areas of the amplified voltage were visible: closer to 400 V and in the range close to 600 V. The greater cell power in the second-generation drive system was a result of the 17% higher current values provided by these cells (cell power values up to I = 350 A are practically the same). The number of cells was reduced by 11% (from 370 to 330), while increasing the cell power density by 92% (from 2.8 to 5.4 kW/kg).

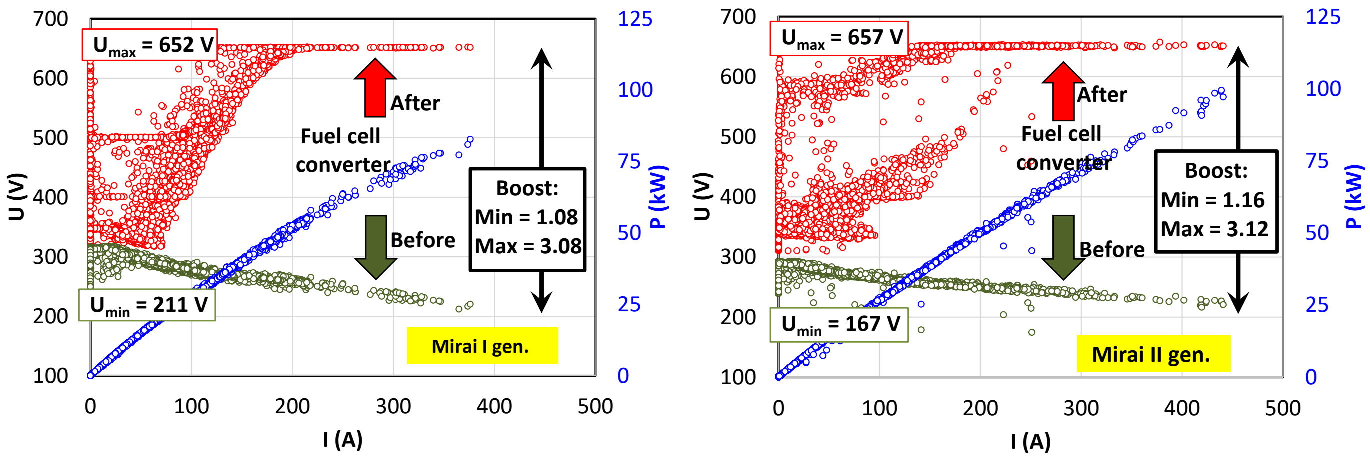

Figure 10. Current-voltage characteristics of a fuel cell stack: (**a**) first-generation drive; (**b**) second-generation drive.

The voltage characteristics of the first-generation converter are steeper (Figure 10): small changes in the input voltage corresponded to a significant change in the output voltage (in the range of 70–200 A). In the case of the second-generation voltage converter, the characteristics of the output voltage changes are shifted towards higher current values (in the range of 100–230 A).

A more detailed analysis of the voltage and current values relative to the vehicle speed allowed for additional observations (Figure 11). The first converter generation allowed for greater changes in the voltage amplification values in each of the driving sections, i.e., at different driving speeds (Figure 11a). In the urban section, voltage changes in the range of 330–500 V were observed. In the field of rural and motorway driving, the changes achieve maximum values of voltage amplification equal to 650 V.

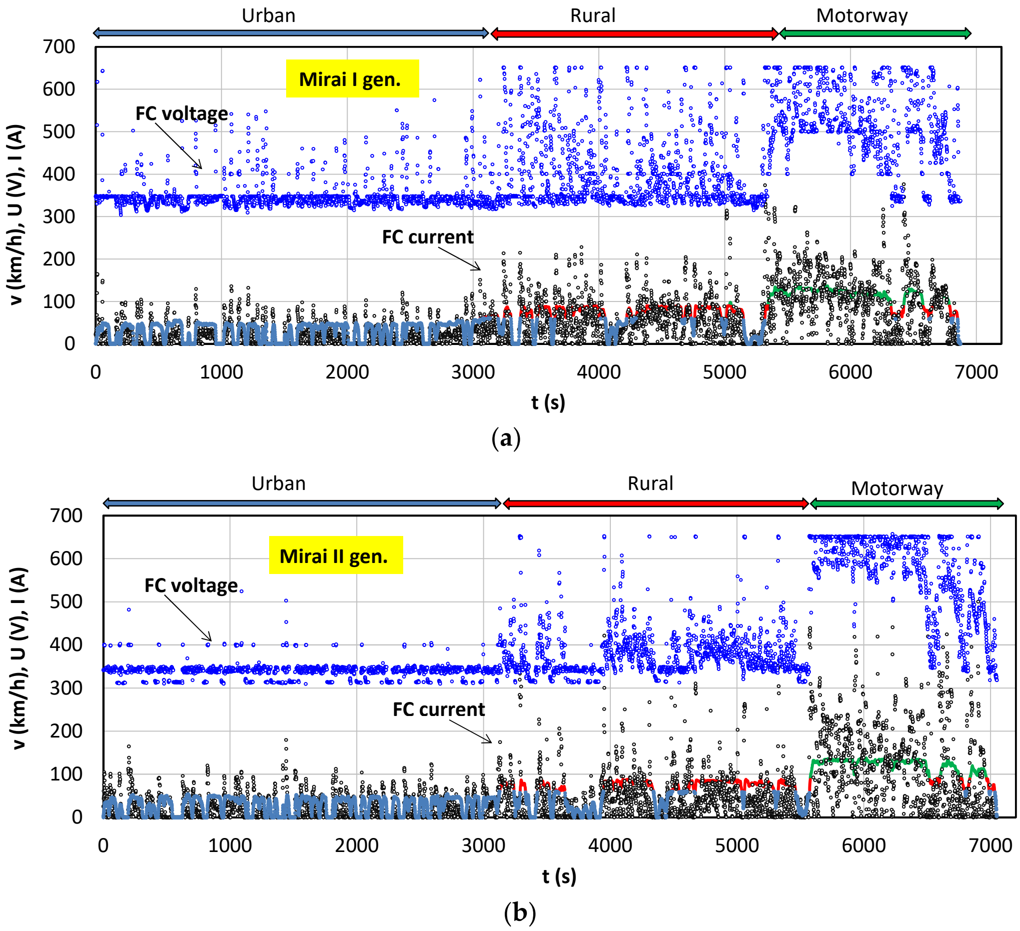

Figure 11. Voltage and current characteristics of the fuel cell converter depending on the speed profile: (**a**) first-generation FC; (**b**) second-generation FC.

The converter of the second-generation drive system enabled a slightly different form of control: in the urban section, the maximum voltage amplification values were limited to about 400 V, while in the rural section, they were 330–500 V (where high values appeared sporadically)—see Figure 11b. The maximum voltage gain values appeared only in the motorway driving section. Such changes in voltage control resulted in the appearance of two characteristic conversion areas in the second-generation system.

Analyzing the electric motors operating conditions for both generations of drives showed how different those operating conditions were. The usable speed range of the first-generation engine was 20% more narrow than that of the second generation (maximum engine speeds of both generations were higher by about 3500 rpm)—see Figure 12. Despite the 10% smaller maximum torque value of the second-generation engine, its power was 10% greater (with 50% greater rotational speed at the same time).

The maximum voltage amplification values (650 V) occurred in similar areas of the electric motor operation characteristics for both generations. The total shares of the engines operating time were slightly different: the first-generation drive system showed a greater share of the engine operation during the tests. In the second generation of the drive, the share of regenerative braking increased, reaching 24% to 16% in the first generation. The second-generation engine had a slightly smaller maximum braking torque (100 Nm compared to 125 Nm), but its rotational speed range was significantly larger: 1000–4000 rpm compared to the first-generation drive engine (1000–2000 rpm). Such changes can only partially be explained by the speed increase in the second-generation engine.

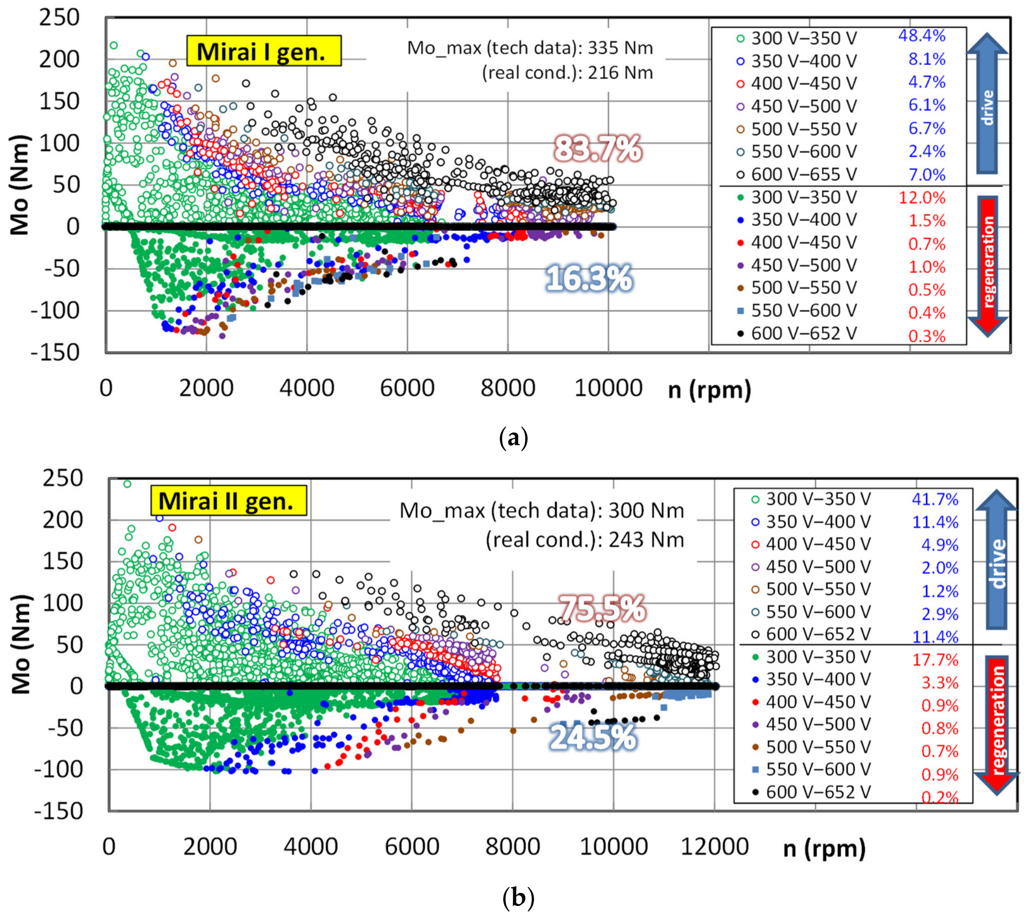

Figure 12. Electric motor characteristics (propulsion and regenerative braking) with supply voltage ranges and operating time density: (**a**) first-generation drive; (**b**) second-generation drive.

Figure 13 represents an assessment of the cooperation between the fuel cell and the battery system. It shows that the first-generation control system was characterized by a significant share of the cell's power in relation to the battery. The area representing a greater use of battery power than fuel cell power is minimal and is not significantly impactful. At high cell powers, the battery power was low and applied on average to power in the range of up to 10 kW (Figure 13a). With regard to the second generation of the drive, the area of the graph for which the relationship Ne_BATT > Ne_FC was satisfied is much larger. There is a significant share of points where the battery power was twice the power provided by the fuel cell. This type of operation did not occur in the first-generation drive system. As previously mentioned, this was a result of using a new generation Li-ion battery. Although the maximum declared battery powers were stated as 25.5 and 31.5 kW, respectively, such values are not commonly observed when analyzing the drive systems in operation during drive tests.

Due to the lower FC power in the first-generation drive, a greater use of the battery power was observed with an average cell load. The FC-BATT operation characteristics in the second-generation drive system were different: the cooperation of both systems was found to be in the cell power range up to 40 kW. In this range, the use of the battery was notable (on average up to 10 kW). At higher cell power values, the battery was used in a fairly narrow range of power (±3 kW)—see Figure 13b.

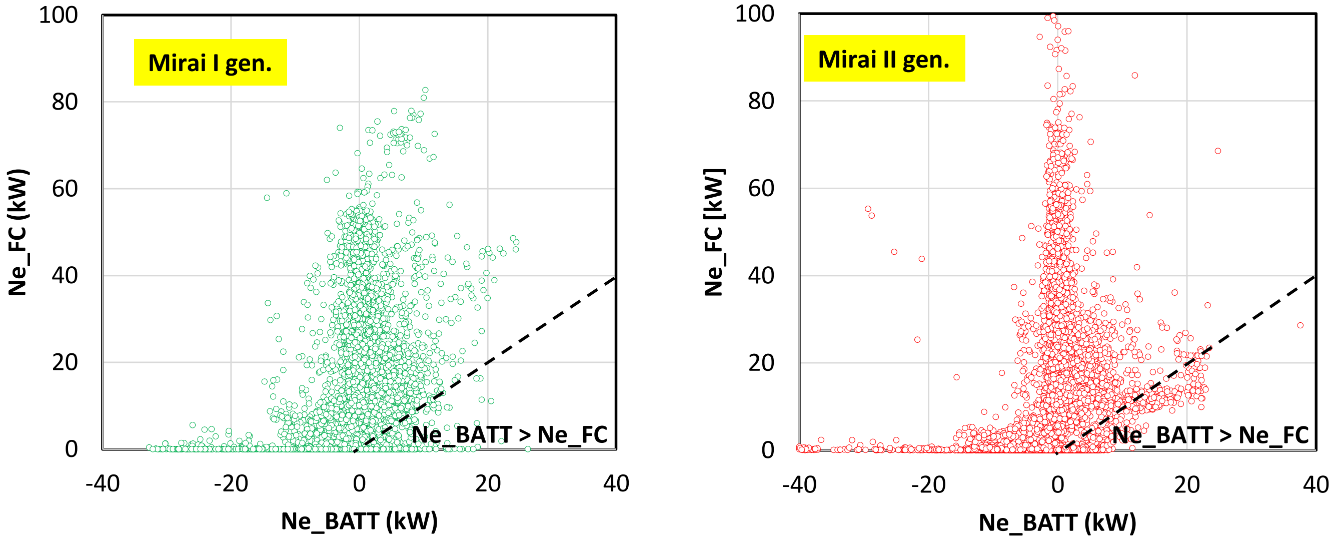

(**a**) (**b**)

Figure 13. Share of use between the fuel cell and the battery: (**a**) first-generation drive; (**b**) second-generation drive.

It should be noted that the changes from one drive system generation to another do not lead to significant differences in the use of battery power and fuel cell power (which is also shown in Figure 11). In urban driving conditions, the second generation of the drive was characterized by higher battery power values (during discharging and charging). This was mainly due to the increased total mass of the vehicle. Nevertheless, the share of fuel cell power was almost constant (the difference was 5%, which is not a significant change). The changes in the mean battery power (during charging and discharging) between vehicle generations amounted to 25% (where higher values were observed for the newer generation drive)—see Figure 14. The battery in the first-generation drive was used on average in a range of 2.6–4.6 kW (irrelevant of the vehicle speed), while for the second-generation drive, it was used in a range of 4.2–4.7 kW. In this respect, there is a link between the driving speed and the battery power used (higher driving speed relating to more power drawn from the battery). Both generations of the drive systems used the battery mostly in the power range from 0 to 5 kW, but it should be noted that there was a variation, where at the maximum driving speeds, the share of the battery was the smallest (Figure 14).

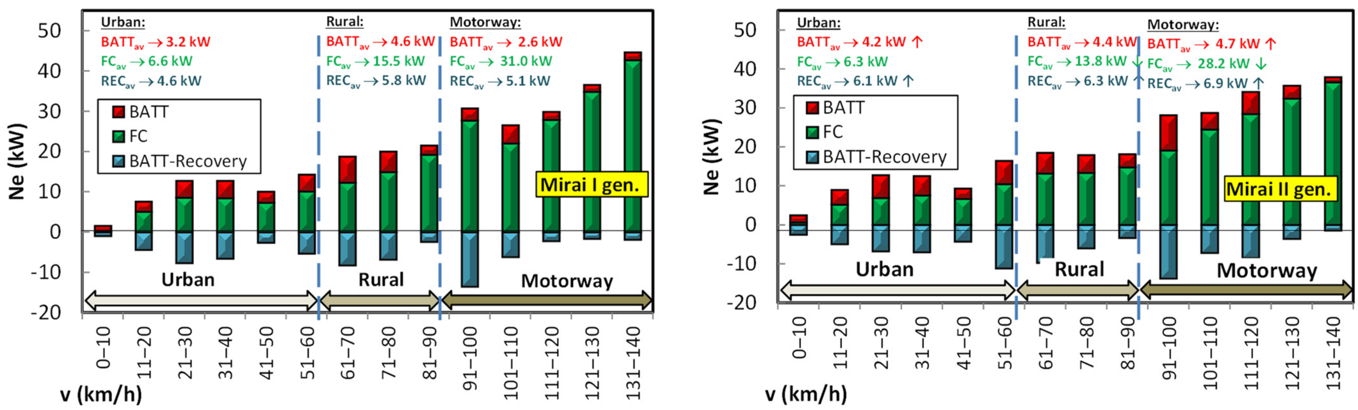

(**a**) (**b**)

Figure 14. Mean battery and fuel cell power values assigned between respective vehicle the speed ranges; additionally, the mean data on the respective powers were given, broken down into the test drive sections: (**a**) for the first generation of the drive; (**b**) for the second generation of the drive.

The mean power provided by the fuel cell in urban driving mode was twice that of the battery. This property was the same for both generations of the drive system. It could be noted that despite the greater mass of the second-generation vehicle, the mean power drawn from the fuel cell in rural and motorway mode was lower. This indicates that the energy management system in the vehicle was more modern (despite the use of similar battery power). The mean cell power was twice as large as in rural driving conditions in motorway driving. The ratio of medium powers in rural and urban modes in both generations was almost 2.

In both drive systems generations, the energy recovery in the individual driving sections was greater than the power consumption from the battery. In urban driving, this ratio was 1.4:1 (recovery to power consumption) for both tested generations. The power values in the newer generation were overall greater. In both drive systems, the highest values of recovered power were observed within the speed range of 90–100 km.

6. Energy Flow

The energy flow analysis was performed in accordance with the conditions presented in the Materials and Methods chapter.

The battery energy in both drive generations accounted for a small share of the total energy used by the vehicle drive (irrespective of which drive system generation was tested). Regardless of the drive section, the share of the battery power in the vehicle drive was approximately 1%. This value was also independent of the generation of the drive system. Additionally, in both generations, the share of the use of the fuel cell was significantly increasing (which was also suggested by the increasing α angles—see Figure 15a,b). The mean value of the battery energy used in the first-generation drive varied from 100 Wh/100 km in the urban section to 200 Wh/100 km in the motorway section. In the second-generation drive, these values were about 25% lower.

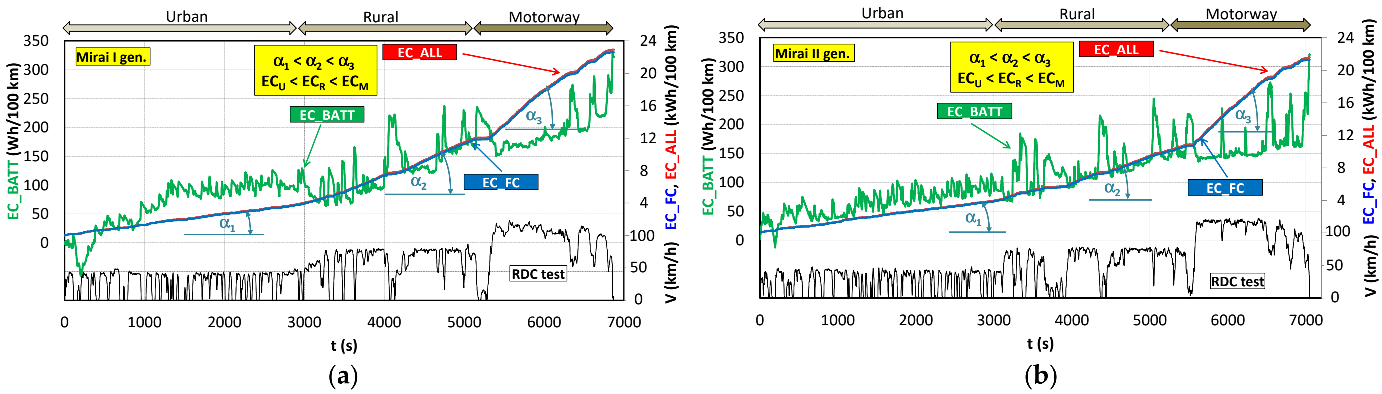

Figure 15. The use of battery and fuel cells energy in road tests of both generations of Toyota Mirai drives: (**a**) first generation; (**b**) second generation.

The conducted research concluded with the total energy consumption of the hydrogen propulsion systems being determined. The analysis of Figure 16 showed that the first-generation system in relation to the second generation had lower battery energy consumption in the urban section. This difference was about 30%. In the next section, these differences were smaller (in the rural section, the use of the battery by the first-generation drive system was lower by only 10%). The use of a fuel cell was more significant in the second-generation system. In the urban section, it was 3% higher, while in the rural section, it was 20% lower (despite the much greater vehicle mass). The total energy consumption of the second-generation drive fuel cell was 6% lower (with a 30% higher battery energy consumption and 27% more energy recovered).

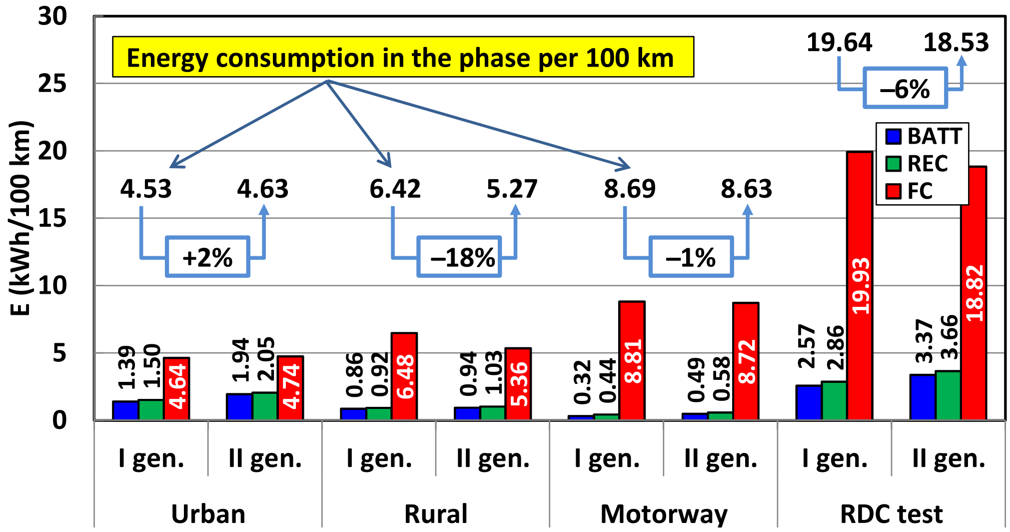

Figure 16. Energy consumption values for both generations of Toyota Mirai drive in individual test drive sections as well as throughout the whole test (the height of bars corresponds to energy from the battery, energy recovered and energy from the fuel cell).

The analysis of the total energy consumption ($E_{FC} + E_{BATT} - E_{REG}$) indicates that a higher consumption for the new generation drive only occurred in the first (urban) driving section. Each subsequent section resulted in lower energy consumption. The greatest differences were recorded in the rural section (due to significant differences in fuel cell energy consumption). The total difference in the RDC test was 6% in favor of the second-generation drive.

The total energy consumption appears in favor of the second-generation drive, although that is not very obvious. The previously demonstrated differences exist but require further analysis. Based on the data from Table 1, it is necessary to indicate a 30% increase in the mass of the vehicle for the second-generation drive. The inclusion of this data in relation to the energy consumed would allow for a more comprehensive comparison of the tested drives.

Taking into account the above-mentioned mass increase for the second-generation vehicle, the specific energy (energy related to the unit of vehicle mass) was calculated for each test section and for the entire RDC test (Figure 17). By using such a variable, a reduction in energy consumption in the second-generation drive was achieved for each of the test sections. In the urban section, this reduction was 22%. In this case, the relation between the sum of the specific energies of the cell and the battery after subtracting the energy from regenerative braking was calculated. By using this approach, the greatest energy reduction was observed in the rural section of the test drive (by about 37%). The total energy reduction in the RDC test was 28%. The analysis of the three energy components (FC, BATT and REG) shows that the most significant changes in the overall RDC test relate to the reduction of the specific energy of the fuel cell (by almost 30%). The battery specific energy consumption throughout the test was the same (despite slight differences in the individual drive sections of the test). The second generation of the drive was also characterized by a slightly lower energy recovery, of 3% (but in absolute values, it was almost 30% greater—see Figure 15).

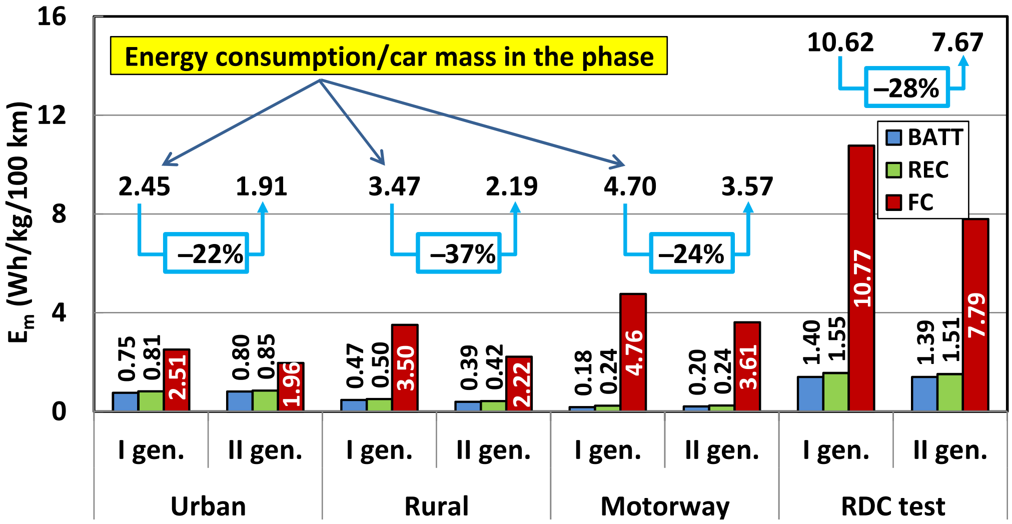

Figure 17. Energy consumption values relative to the vehicle mass determined for both drive generations of the Toyota Mirai in individual test sections as well as for the entire test (the height of the bars correlates to the specific energy from the battery, energy recovered with braking and energy from the fuel cell).

7. Future Work

The analysis of future generations of hydrogen propulsion systems is not exhaustive with the current analyses. Further work will focus on:

1. Detailed analysis of the functioning of fuel cells and their response rate to load changes due to traffic conditions
2. Evaluation of the rate of degradation of fuel cells with regard to the analysis of activation losses, resistance losses and mass transport losses.

These tests are particularly important, not for the registration test, but for the road test, which best reflects real traffic conditions.

8. Conclusions

The analysis of both generations of hydrogen drives resulted in reaching the following conclusions based on real road tests:

1. As the driving speed increased in the successive test sections, the battery SOC decreased (based on Figure 6). This means that the battery was not recharged to its initial values. The use of a Li-ion battery in the second-generation system enabled much wider limits of SOC changes: about 16% (only 7% for the first generation). Although these changes were quite different in nature, the mean values of SOC drop regardless of the drive generation were 3%.
2. The different types of batteries used in the two drive generations meant that their charging powers were also different. The second-generation drive enabled 28% greater power recovery (max 42 kW) than the first-generation system (this was achieved thanks to the voltage values being higher by 3% and the current intensity higher by 20%). Despite the different energy storage systems, their discharge during the tests took place with the same maximum power of about 26 kW.
3. The fuel cell voltage converter in the second-generation system worked differently than that in the first generation. In the latest generation of the hydrogen drive system, the maximum voltage values were achieved only in motorway driving sections. In the urban section, the second-generation system limited the voltage to about 400 V (first generation—up to 500 V).
4. The higher maximum rotational speed of the second-generation electric motors (by 20%) did not translate into changes in the voltage value in individual operating

points. Despite the lower maximum torque value in the second-generation engines (by 11%), the actual value of the useful torque was 12% greater. The second-generation engine had a slightly smaller maximum braking torque value (100 Nm as compared to 125 Nm), but the rotational speed range was significantly larger: 1000–4000 rpm compared to the first-generation drive (1000–2000 rpm).

5. The mean value of the fuel cell power in the urban driving section was twice that of the battery. This was true for both generations of the drive. Despite the greater mass of the second-generation vehicle, the mean power of the cell in rural and motorway sections was lower. This was a sign of a more modern energy management system in the newer vehicle (despite using similar battery power). In motorway driving, the mean cell power was double the value it reached in the rural driving section.
6. The mean battery energy value in the first-generation drive ranged from 100 Wh/100 km in the urban section up to 200 Wh/100 km in the motorway test section. For the second-generation drive, these values were about 25% lower. The energy consumption in the RDC test of the first-generation drive was 19.63 kWh/100 km. This was 6% more than for the second-generation drive (despite the 30% greater mass of the second-generation vehicle).
7. It is necessary to consider the specific energy for both vehicles, which takes into account the differences in the mass of both generations of vehicles. Despite the more favorable absolute energy ratios (E), the specific energy values (E_m) proved to be a more accurate indicator when comparing the two drive systems.
8. The research confirms that passenger FCEV is one of the most mature and sophisticated hydrogen technology in comparison to other mobility solutions. Simultaneously, we found arguments that current technology still improves what means that learning rates becoming positive contributing to technology improvement.

Author Contributions: Conceptualization, I.P. and A.S.; methodology, I.P., A.S. and G.T.; software, I.P.; validation, I.P., A.S. and G.T.; formal analysis, I.P. and A.S.; investigation, I.P.; resources, A.S.; data curation, I.P., A.S. and G.T.; writing—original draft preparation, I.P., A.S. and G.T.; writing—review and editing, I.P., A.S. and G.T.; visualization, I.P. and G.T.; supervision, I.P.; project administration, I.P. and A.S. All authors have read and agreed to the published version of the manuscript.

Funding: This research received no external funding.

Institutional Review Board Statement: Not applicable.

Informed Consent Statement: Not applicable.

Data Availability Statement: The data presented in this study are available on request from the corresponding author.

Conflicts of Interest: The authors declare no conflict of interest.

References

1. Fitzmorris, D. A carbon intensity analysis of hydrogen fuel cell pathways. *SAE Int. J. Adv. Curr. Prac. Mobil.* **2021**, *3*, 1317–1322. [CrossRef]
2. Zaccardi, J.-M.; Pilla, G. Hydrogen as a combustion enhancer for highly efficient ultra-lean spark-ignition engines. *SAE Int. J. Adv. Curr. Prac. Mobil.* **2020**, *2*, 401–414. [CrossRef]
3. Molina, S.; Novella, R.; Pla, B.; Lopez-Juarez, M. Optimization and sizing of a fuel cell range extender vehicle for passenger car applications in driving cycle conditions. *Appl. Energy* **2021**, *285*, 116469. [CrossRef]
4. Wilberforce, T.; El-Hassan, Z.; Khatib, F.N.; Al Makky, A.; Baroutaji, A.; Carton, J.G.; Olabi, A.G. Developments of electric cars and fuel cell hydrogen electric cars. *Int. J. Hydrogen Energy* **2017**, *42*, 25695–25734. [CrossRef]
5. Taner, T. The novel and innovative design with using H2 fuel of PEM fuel cell: Efficiency of thermodynamic analyze. *Fuel* **2021**, *302*, 121109. [CrossRef]
6. IEA. *World Energy Outlook 2021*; IEA: Paris, France, 2021; Available online: https://www.iea.org/reports/world-energy-outlook-2021 (accessed on 18 November 2021).
7. Dawood, F.; Anda, M.; Shafiullah, G.M. Hydrogen production for energy: An overview. *Int. J. Hydrogen Energy* **2020**, *45*, 3847–3869. [CrossRef]

8. Gunarathna, M.A.C.L.; Yang, R.J.; Song, A. Diverse distributed renewable energy trading paradigms: A business model review. *J. Environ. Plan. Manag.* **2022**, *65*, 1–36. [CrossRef]
9. Leisner, P.; Johansson, E. Aspects to be considered when making innovation out of promising research results in surface technology. *Trans. IMF* **2019**, *97*, 67–72. [CrossRef]
10. Bruce, S.; Temminghoff, M.; Hayward, J.; Schmidt, E.; Munnings, C.; Palfreyman, D.; Hartley, P. *National Hydrogen Roadmap*; CSIRO: Canberra, Australia, 2018; Available online: http://www.csiro.au (accessed on 15 November 2020).
11. Kupecki, J. (Ed.) *Analysis of the Potential of Hydrogen Technologies in Poland until 2030 with a Perspective until 2040*; The National Fund for Environmental Protection and Water Management: Warsaw, Poland, 2021.
12. Tchorek, G.; Kozioł, W.; Wójtowicz, S.; Targowski, F.; Grzybowski, M. Hydrogen economy value chain. In *Energy and Climate Transformation—Selected Dilemmas and Recommendations*; Nowak, A.Z., Kurtyka, M., Tchorek, G., Eds.; University of Warsaw: Warsaw, Poland, 2021. [CrossRef]
13. Fan, I.; Tu, Z.; Chan, S.H. Recent development of hydrogen and fuel cell technologies: A review. *Energy Rep.* **2021**, *7*, 8421–8446. [CrossRef]
14. Hong, B.K.; Kim, S.H. Recent advances in fuel cell electric vehicle technologies of Hyundai. *Elec. Soc. Trans.* **2018**, *86*, 3–11. [CrossRef]
15. Jiao, K.; Xuan, J.; Du, Q.; Bao, Z.; Xie, B.; Wang, B.; Zhao, Y.; Fan, L.; Wang, H.; Hou, Z.; et al. Designing the next generation of proton-exchange membrane fuel cells. *Nature* **2021**, *595*, 361–369. [CrossRef] [PubMed]
16. Habibnia, M.; Shirkhani, M.; Tamami, P.G. Optimization of proton exchange membrane fuel cell's end plates. *SN Appl. Sci.* **2020**, *2*, 1380. [CrossRef]
17. Yoshizumi, T.; Kubo, H.; Okumura, M. Development of high-performance FC stack for the new MIRAI. In *SAE Technical*; SAE International: Warrendale, PA, USA, 2021. [CrossRef]
18. Volume Manufacturing of PEM FC Stacks for Transportation and in-line Quality Assurance. European Commission. 2019. Available online: https://cordis.europa.eu/project/id/671465 (accessed on 1 November 2021).
19. Fuel Cells and Hydrogen 2 Joint Undertaking (FCH 2 JU). 2019 Annual Work Plan and Budget (FCH 2 JU, 2018). Available online: https://ec.europa.eu/research/participants/data/ref/h2020/other/wp/jtis/h2020-wp19-fch_en.pdf (accessed on 1 November 2021).
20. Gößling, S.; Nickig, N.; Bahr, M. 2-D + 1-D PEM fuel cell model for fuel cell system simulations. *Int. J. Hydrogen Energy* **2021**, *46*, 34874–34882. [CrossRef]
21. Murschenhofer, D.; Kuzdas, D.; Braun, S.; Jakubek, S. A real-time capable quasi-2D proton exchange membrane fuel cell model. *Energy Convers. Manage.* **2018**, *162*, 159–175. [CrossRef]
22. Wu, K.; Xie, X.; Wang, B.; Yang, Z.; Du, Q.; Xuan, J.; Zu, B.; Liu, Z.; Jiao, K. Two-dimensional simulation of cold start processes for proton exchange membrane fuel cell with different hydrogen flow arrangements. *Int. J. Hydrogen Energy* **2020**, *45*, 17795–17812. [CrossRef]
23. Arif, M.; Cheung, S.C.P.; Andrews, J. Diagnostic analysis of a single-cell Proton Exchange Membrane unitised regenerative fuel cell using numerical simulation. *Int. J. Hydrogen Energy* **2021**, *46*, 29488–29500. [CrossRef]
24. Tsukamoto, T.; Aoki, T.; Kanesaka, H.; Taniguchi, T.; Takayama, T.; Motegi, H.; Takayama, R.; Tanaka, S.; Komiyama, K.; Yoneda, M. Three-dimensional numerical simulation of full-scale proton exchange membrane fuel cells at high current densities. *J. Power Sources* **2021**, *488*, 229412. [CrossRef]
25. Xie, B.; Zhang, G.; Jiang, Y.; Wang, R.; Sheng, X.; Xi, F.; Zhao, Z.; Chen, W.; Zhu, Y.; Wang, Y.; et al. "3D+1D" modeling approach toward large-scale PEM fuel cell simulation and partitioned optimization study on flow field. *eTransportation* **2020**, *6*, 100090. [CrossRef]
26. Pielecha, I.; Szwajca, F. Cooperation of a PEM fuel cell and a NiMH battery at various states of its charge in a FCHEV drive. *Eksploat Niezawodn.* **2021**, *23*, 468–475. [CrossRef]
27. de Almeida, S.C.A.; Kruczan, R. Effects of drivetrain hybridization on fuel economy, performance and costs of a fuel cell hybrid electric vehicle. *Int. J. Hydrogen Energy* **2021**, *46*, 39404–39414. [CrossRef]
28. Lohse-Busch, H.; Stutenberg, K.; Duoba, M.; Liu, X.; Elgowainy, A.; Wang, M.; Wallner, T.; Richard, B.; Christenson, M. Automotive fuel cell stack and system efficiency and fuel consumption based on vehicle testing on a chassis dynamometer at minus 18 °C to positive 35 °C temperatures. *Int. J. Hydrogen Energy* **2020**, *45*, 861–872. [CrossRef]
29. Technology Assessment of a Fuel Cell Vehicle: 2017 Toyota Mirai. Available online: https://www.anl.gov/d3 (accessed on 1 November 2021).
30. Raeesi, M.; Changizian, S.; Ahmadi, P.; Khoshnevisan, A. Performance analysis of a degraded PEM fuel cell stack for hydrogen passenger vehicles based on machine learning algorithms in real driving conditions. *Energy Convers. Manag.* **2021**, *248*, 114793. [CrossRef]
31. Changizian, S.; Ahmadi, P.; Raeesi, M.; Javani, N. Performance optimization of hybrid hydrogen fuel cell-electric vehicles in real driving cycles. *Int. J. Hydrogen Energy* **2020**, *45*, 35180–35197. [CrossRef]
32. Ferrara, A.; Jakubek, S.; Hametner, C. Energy management of heavy-duty fuel cell vehicles in real-world driving scenarios: Robust design of strategies to maximize the hydrogen economy and system lifetime. *Energy Convers. Manag.* **2021**, *232*, 113795. [CrossRef]

33. Xu, L.; Li, J.; Ouyang, M. Energy flow modeling and real-time control design basing on mean values for maximizing driving mileage of a fuel cell bus. *Int. J. Hydrogen Energy* **2015**, *40*, 15052–15066. [CrossRef]
34. Szałek, A.; Pielecha, I.; Cieslik, W. Fuel cell electric vehicle (FCEV) energy flow analysis in real driving conditions (RDC). *Energies* **2021**, *14*, 5018. [CrossRef]
35. Konno, N.; Mizuno, S.; Nakaji, H.; Ishikawa, Y. Development of compact and high-performance fuel cell stack. *SAE Int. J. Altern. Power.* **2015**, *4*, 123–129. [CrossRef]